WORLD JOURNAL OF PHARMACEUTICAL RESEARCH
SJIF Impact Factor 8.074
Volume 7, Issue 8, 461-475. Conference Article ISSN 2277– 7105

S-ALIZARIN RED DYE REMOVAL FROM AQUEOUS SOLUTION USING NANOCHITOSAN/IRON OXIDE NANOPARTICLES/TAMARIND SHELL BLEND

E. Jothi and Vijayalakshmi K.*

PG and Research Department of Chemistry, D.K.M College for Women, Vellore, Tamilnadu, India.

Article Received on
05 March 2018,
Revised on 25 March 2018,
Accepted on 15 April 2018
DOI: 10.20959/wjpr20188-11166

***Corresponding Author**
Dr. Vijayalakshmi K.
PG and Research Department of Chemistry, D.K.M College for Women, Vellore, Tamilnadu, India.

ABSTRACT

The present research work deals with removal of S-Alizarin red dye from aqueous solution using nanochitosan/iron oxide nanoparticles/tamarind shell ternary blend in batch mode on laboratory scale. The effect of contact time on the adsorptive removal efficiencies was investigated and the obtained results indicate that around 75% s-alizarin red dye were removed from the aqueous solution. In addition the kinetic studies reveals that the pseudo second order kinetic model is followed and hence from the observed results it was suggested that the prepared nanochitosan/iron nanoparticles/tamarind shell ternary blend acts as a very good adsorbent for dye effluent treatment at the industrial level.

KEYWORDS: nanochitosan, tamarind shell, iron oxide nanoparticles, adsorption, s-alizarin red dye.

INTRODUCTION

Disruption and gradual destruction of the aquatic ecosystem occurs by the dye-bearing wastewater which is not only aesthetically displeasing but also restrains sunlight from penetrating into the aquatic system.[1] The increasing dye pollution occurs mainly due to the intensive technological and industrial development and this is because of the disposal of wastewaters from different industries, for example textile, leather, plastics and cosmetics.[2] Even after the conventional removal processes, one of the most difficult wastewater to treat is the dye wastewater from textile and dyestuff industries since the colour tends to hold so

strongly.[3] Annually around 700,000 tons of more than 100,000 commercially available dyes were produced.[4] The presence of some of these dyes even in very minor amounts i.e. < 1 $mg.dm^{-3}$ are so harmful leading to serious health disorders.

Among the most commonly used dyes, alizarin red is selected for treatment purpose in this study due to the following reasons. Alizarin Red S, belongs to the group of an anthraquinone dye and due to its complex structures of the aromatic rings it cannot be completely degraded by general physicochemical and biological processes which can afford high physicochemical, thermal and optical stability.[5] Due to its complex structures of the aromatic rings, the S Alizarin red turns to be a potential toxic to the biota and aquatic life leading to several harmful effects such as gastritis, mal-functioning of lungs, severe headache, painful micturition and methemoglobinemia.[6] Several physicochemical methods were utilized for the treatment of dyes[7][8] such as coagulation, floatation, precipitation and biosorption process.

Among the various effective routes of treatment, the biosorption has received considerable attention and hence in this present study, this bisorption process has been adopted since it has the potential to become an efficient, clean and cheap technology for the wastewater treatment.[9] Different kinds of adsorbents such as metal oxides, activated carbon, clays, charcoal, activated carbon, agrowaste, fruit shell, nanoparticles, biopolymers, alumina, calcium oxide, cynodon dactylon have been used for treatment purpose. Activated carbon is the most typically used adsorbent for the color removal[10] and this was due to its functionality for efficaciously adsorbing a wide range of materials.[11] Eventhough it has greater adsorption capacity, its utilization for dye removal is restricted due to its high cost and difficulty in its regeneration. When compared to the commercial highly efficient activated carbon, the use of synthetic iron oxide nanoparticles is much more economic and hence many researchers have focused on investigating the capabilities of magnetic nanoparticles as an efficient adsorbent which is having large specific surface area and small diffusion resistance.[12] Zhu and his coworkers reported about the use of magnetic cellulose/Fe_3O_4/activated carbon composite as adsorbent for for removal of Congo red dye.[13]

Due to their large surface area, adsorption capacity and heat or chemical resistance properties for the removal of contaminants in aquatic environments, the nanochitosan has been chosen as an adsorbent for dye removal processes in many research works. This nanochitosan biopolymer has become a more environmentally friendly substance of choice due to its

excellent physicochemical properties and non toxic nature.[14] Razavi and her coworkers investigated the removal of Congo red dye from aqueous solutions using nanochitosan as adsorbent. Results showed that under optimal conditions the nanochitosan is able to remove maximum amount of Congo red from aqueous solutions.[15] Also the performance of nanochitosan as an adsorbent to remove acid orange 10 (AO10), acid orange 12 (AO12), acid red 18 (AR18) and acid Red 73 (AR73) from aqueous solution has been investigated by Cheung and his coworkers.[16]

In India, the agricultural waste like tamarind pod shell is discarded as waste and since it is available free of cost, it is used for wastewater treatment. The utilization and recycling of this waste for wastewater treatment would not only be economical but also help to solve waste disposal problems. Removal of methylene blue and amaranth dye from aqueous solution using tamarind pod shells has been investigated by Ahalya and her coworkers. Results showed that the tamarind pod shell was found to be an effective adsorbent for the removal of methylene blue and amaranth dye from aqueous solution.[17] Hence in the present research work, based on literature survey, three materials namely nanochitosan, iron oxide nanoparticles and tamarind shell were selected to prepare the ternary blend. We had examined the removal of alizarin red dye onto nanochitosan/iron oxide nanoparticles/tamarind shell as adsorbent. The main objectives of the current study are to study the chemistry of S Alizarin red dye biosorption onto nanochitosan/iron oxide nanoparticles/tamarind shell ternary blend. In addition, the effect of contact time was performed and the kinetic experimental data required for the design and operation of batch reactors were evaluated and investigated.

MATERIALS AND METHODS

Materials

The natural agro waste *Tamarindusindica* pod shells collected from Vellore area, India. The biopolymer chitosan was purchased from Indian Sea Foods, Cochin, Kerala. Certain chemicals namely sodium tripolyphoshate, glacial acetic acid, oxalic acid, ferrous sulphate and polyvinyl alcohol was procured from Nice Chemicals Pvt Ltd, Thomas Bakers Pvt Limited, Sisco Research Laboratories Pvt Ltd. The reactive basic dye S-Alizarin red used in the present research work has the molecular formula ($C_{14}H_7NaO_7S$), molecular weight of 240g/mol and wavelength of maximum absorbance of 480 nm and was supplied by S.D Fine

Chemicals Private Limited, Mumbai. All the chemical used in the present research work were of analytical grade.

Preparation of nanochitosan

Through ionic gelation method, in the present research work, the nanochitosan can be prepared by the interaction of oppositely charged macromolecules (positively charged chitosan macromolecule with the anionic tripolyphosphate).[18] Homogeneous chitosan solution was synthesized by dissolving 1g of chitosan in 200 ml of 2% acetic acid solution prepared in deionized water. Followed by this, the complete stirring process was done for about 15 minutes. The dropwise addition of sodium tripolyphosphate solution (0.8g of TPP (sodium tri poly phosphate) dissolved in 107ml of deionized water) to chitosan solution has been carried out and this solution mixture was then allowed to stir well using magnetic stirrer for a period of 30 minutes. A milky emulsion like appearance of nanochitosan obtained was then allowed to settle for 24 hours, mother liquor is decanted and the milky suspension like substance settled at the bottom (NCS) of beaker is kept in a freezer and stored for further use.

Preparation of tamarind shell

The tamarind fruit shells were collected from the natural tamarind trees. The tamarind fruit shells were cleaned with distilled water and then sun dried for 48 hours. The dried tamarind shell was then grounded, powdered and sieved well to get uniform sized particles. The tamarind shell powder so obtained was then washed thoroughly with distilled water and dried well in the hot air oven for 24 hours at 80ºC. Finally the tamarind fruit shell powder is stored in airtight plastic bottles for further use. The photograph of the prepared tamaring shell powder was shown below (Fig.A).

Preparation of iron oxide nanoparticles by hydrothermal method

The iron oxide nanoparticles were synthesized using low temperature combustion method by employing iron oxalate as precursor. As per the method reported by Priscilla Prabhavathi and

her coworkers[19] by utilizing the hydrothermal method, in two satges, the iron oxide nanoparticles can be prepared as follows:

Stage: 1- Synthesis of Iron oxalate Precursor

Equimolar proportions say, 0.25g of Ferrous sulphate and oxalic acid is dissolved in minimum volume of water and stirred for 15 minutes on a magnetic stirrer. Yellow precipitate for iron oxalate dehydrate obtained is then filtered washed with distillied water and finally dried with acetone. The photograph of the prepared iron oxalate precursor was represented below (Fig.B).

Fig.B: Photograph of Iron oxalate.

Stage: 2- Synthesis of iron oxide nanoparticles

The above prepared iron oxalate precursor was mixed with polyvinyl alcohol in the weight ratio of 1:5. The resultant mixture was then powdered well in a mortar, mixed in a silica crucible and ignited in an electric furnace and while heating, the temperature should not exceed 300°C. During the heating process, initially the PVA is melted, then frothed and finally undergoes complete ignition process leading to give iron oxide as residue. The obtained sample (iron oxide residue) is then calcinated at 110°C for 4 hours to remove impurities and the iron oxide nanoparticles was then cooled, dried and powdered for further use. The photograph of the prepared iron oxide nanoparticles was represented below (Fig.C)

Fig. C: Photograph of iron oxide nanoparticles.

Preparation of nanochitosan/iron nanoparticles/tamarind shell blend

Equimolar proportions of the above prepared nanochitosan, iron oxide nanoparticles and tamarind shell powder (1:1:1) taken in a beaker were dissolved in minimum amount of distilled water (10 ml). This solution mixture was then stirred well completely for a period of 30 minutes using magnetic stirrer. And after this stirring process is over, this ternary blended mixture was then poured into petri plates, allowed to dry and then stored in air tight box for further use as biosorbent.

Batch Adsorption studies

The adsorption experiments were carried in a batch process at room temperature by using an aqueous solution of S-alizarin red dye.

Preparation of s-alizarin red dye solution (adsorbate)

A stock solution of S-Alizarin red dye (1000 mg/ L) was prepared by dissolving 1.0 g of it in 1000 ml of distilled water. The pH of the solutions was adjusted using sodium hydroxide and hydrochloric acid and it was suitably diluted to the required initial concentration (200 ppm). The concentration of the dye remaining after adsorption process was determined at 480 nm, using photoelectric colorimeter (Perkin-Elmer Lambda 25).

Experimental method

An accurately weighed amount (0.1g) of nanochitosan/iron nanoparticles/tamarind shell blend (adsorbent) was added to 100ml of the S-Alizarin Red dye solution (adsorbate) taken in stopper conical flask. But before mixing the adsorbate (S-Alizarin Red solution) with the adsorbent, the initial pH of each solution was adjusted to the required value by adding 2N NaOH solution for increasing the pH and 1:1 HCl for decreasing the pH. The above solution mixture was agitated in the shaker for a definite time at a room temperature.

After this shaking process is over, the above mixture was filtered using Whatmann filter paper no.41. The filtered solution ie filterate collected was then analysed for the S Alizarin red adsorption using the photoelectric colorimeter technique. The biosorption studies were carried out with the same procedure in batch mode to identify the effect of contact time (60 min - 300 min) on the biosorption of S-Alizarin Red. The percentage of dye removal was calculated by using following equation respectively

$$\text{Removal}\,(\%) = \frac{C_o - C_f}{C_o} \times 100$$

Where C_o- Initial concentration of metal ion (mg/L) and C_f - Final concentration of metal ion (mg/L).

CHARACTERIZATION

FT-IR Spectral analysis

The FT-IR spectra of prepared samples were recorded by the 200 FT-IR sp0ectrophotometer in the wavenumber range of 400-4000cm^{-1} with the resolution of 2 cm^{-1} at 25°C during 64 scans.

RESULTS AND DISCUSSION

Fourier Transform IR Spectroscopy

The FT-IR spectroscopy is one of the important analytical methods having the ability to directly monitor the vibrations of the functional groups which characterize molecular structure and govern the course of chemical reactions. This FT-IR spectrum can provide certain structural clues to the overall structure of the unknown substance. The FT-IR spectral details of nanochitosan was shown in Fig.1.

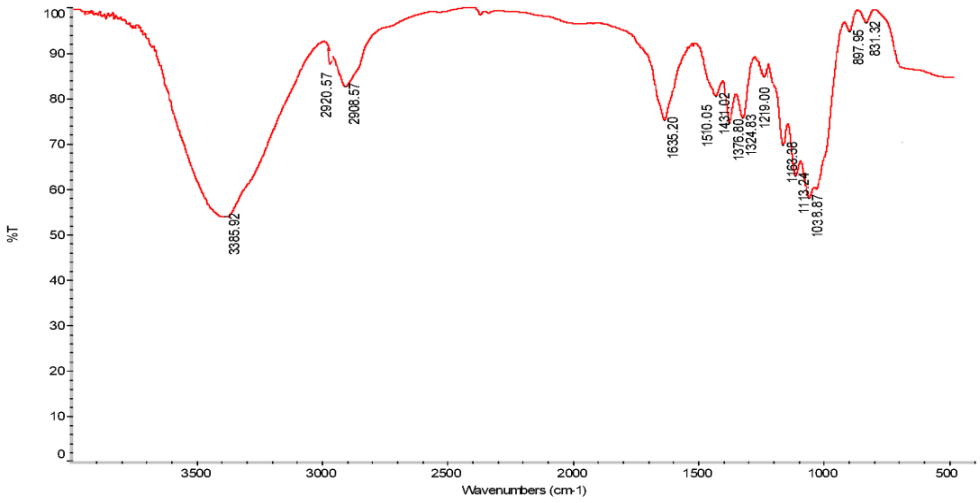

Fig.1: FT-IR spectrum of nanochitosan.

In the FT-IR spectrum of nanochitosan (Fig.1), the strong and wide peak obtained in the 3500-3300 area attributed to hydrogen-bonded O-H stretching vibration (3385.92 cm^{-1}) arising mainly due to physical interactions with TPP. In the same region, the peaks of N-H stretching from primary amine and type II amide have been overlapped.[20] The peaks for asymmetrical and symmetrical stretching in CH_2 group, NH_3^+ stretching, C=O stretching in amides, NH bending and OH in plane bending in alcohols is found at around 2920.57 cm^{-1},

2908.57 cm^{-1}, 1635.23 cm^{-1}, 1510.05 cm^{-1} and 1376.80 cm^{-1}.[21] Also in addition it was identified that in case of nanochitosan, due to the formation of cross links by the interaction of ammonium ion and phosphate ion[22], a P=O absorption band was found to be obtained at 1219.00cm^{-1}. These results have been attributed to the linkage between phosphoric and ammonium ion and hence from the appearance of these peaks it was concluded that the tripolyphosphoric groups of TPP are linked with ammonium groups of chitosan and the inter- and intra-molecular actions are enhanced in nanochitosan.[23]

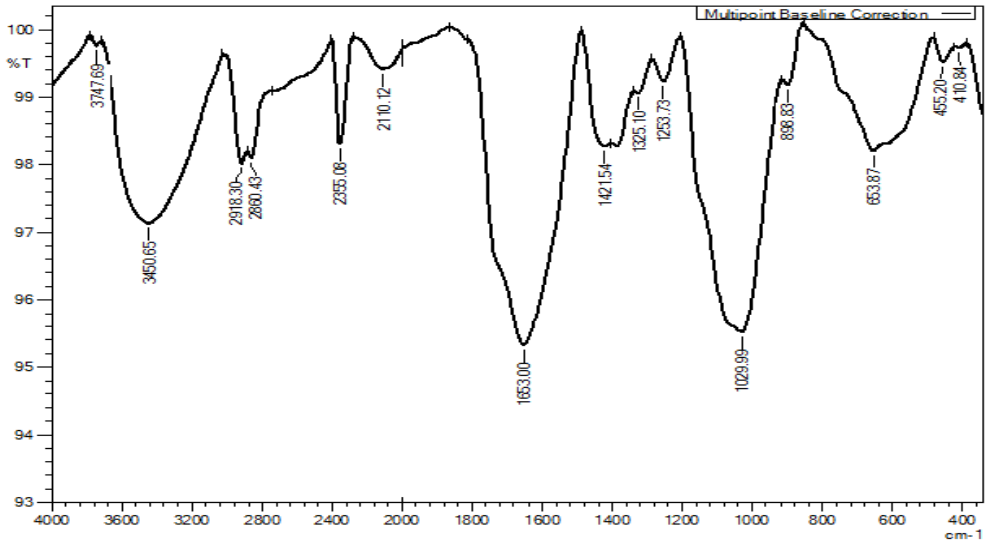

Fig.2: FT-IR spectrum of nanochitosan/iron nanoparticles/tamarind shell blend.

The effective blending of nanochitosan with iron oxide nanoparticles and tamarind shell was confirmed through FT-IR analysis. The FT-IR spectrum of nanochitosan/iron nanoparticles/tamarind shell blend was shown in the Fig.2. The broad absorption band observed at 3450.65 cm^{-1} indicates the presence of surface hydroxyl groups (O–H stretching). The peaks for asymmetrical and symmetrical stretching in CH_2 group and NH_3^+ stretching was found at around 2918.30.57 cm^{-1}, 2860.43 cm^{-1} and 2355.08 cm^{-1}. The absorption band at 1653.00 cm^{-1} is related to the hetroaromatic C-H bond stretching, C=O stretching in acids (tamarind shell) and the C-N stretching is observed at 1421.54 cm^{-1}. The interaction of ammonium ion and phosphate ion in nanochitosan leads to the formation of P=O absorption band at 1253.73 cm^{-1}. Certain absorption bands appearing at 1029.99 cm-1 and 898.83 cm^{-1} was indicative of the C-O stretching and C-C stretching.[24] The band appearing at low wave numbers (< 700 cm^{-1}) are related to vibrations of the Fe-O bonds in iron oxide[25] and the presence of magnetite nanoparticles can be established via the advent of two strong absorption bands around 653.87 cm^{-1} and 585 cm^{-1} respectively. When compared

to the FT-IR spectrum of nanochitosan alone, this nanochitosan/iron nanoparticles/tamarind shell ternary blend shows an extra additional peaks due to the presence of acids and vibrations of the Fe-O bonds in iron oxide. Hence from these additional peaks it was evident that the nanochitosan gets blended effectively with iron nanoparticles and tamarind shell.

Factors influencing the adsorption of S-Alizarin red dye from aqueous solution

In the present study, the effectiveness on the removal of alizarin red dye using nanochitosan/iron oxide nanoparticles/tamarind shell blend as adsorbent by varying contact time was studied and the results were investigated below in detail.

Effect of contact time

The effect of contact time on the adsorption of S- Alizarin Red dye removal from aqueous solution was represented in Fig.3. From Fig.3, it was seen clearly that the maximum adsorption occurred in 30-90 minutes and after 90-120 minutes; an equilibrium state was obtained. Initially due to high concentration gradient and more available adsorption sites, the rate of dye removal is high. The rate of dye removal shows an increased percentage removal with increase in contact time and this process continues until the adsorption process reaches equilibrium. But after reaching equilibrium, ie as the time proceeds no further uptake of adsorbate by adsorbent will occur as time proceeds[26] and this is because of the fact that each adsorbent has limited adsorbent sites. After a certain time, these were exhausted and hence the adsorption process attained an equilibrium state.[27] The above observed overall results conclude that 120 min is fixed as minimum contact time for the maximum removal percent of S-Alizarin Red dye from aqueous solution using nanochitosan/iron oxide nanoparticles/tamarind shell blend as adsorbent.

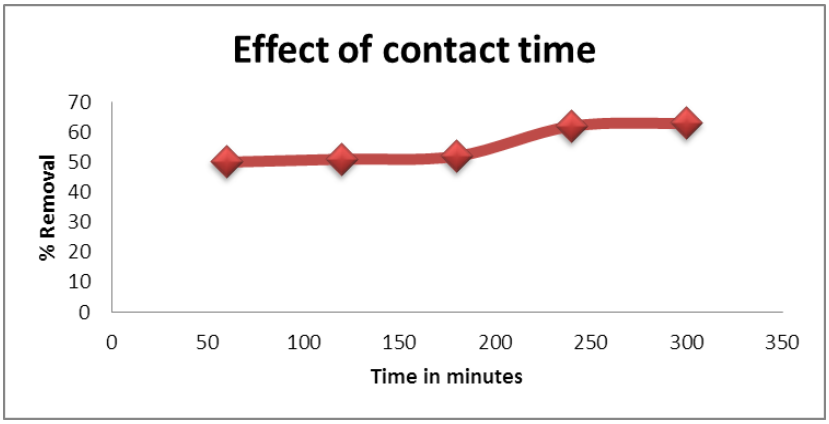

Fig.3: Effect of contact time on the adsorption of S-Alizarin red dye removal from aqueous solution using nanochitosan/iron oxide naoparticles/tamarind shell blend.

Kinetic studies

The kinetic studies were carried out by agitation of 100 mL solutions of S-Alizarin Dye with initial concentrations 200 mg/L and 0.1 g of each adsorbent, at room temperature and at different time intervals from 30 to 150 min. In order to understand the chemical kinetics of solid liquid adsorption process, two kinetic models namely Lagergren pseudo first-order kinetic and pseudo second order kinetic model has been studied.[28] The Larergren model has been effectively used to provide explanation for the adsorption of S-Alizarin red dye onto prepared nanochitosan/iron oxide nanoparticles/tamarind shell blend. The pseudo-first-order rate equation is expressed as follows (Lagergren 1898)

$$\log(q_e - q_t) = \log q_e - \frac{k_1}{2.303} \quad \text{------(1)}$$

Where q_e – equilibrium adsorption capacity (mg/g)

q_t – adsorption capacity after certain time 't'(mg/g)

k_1 is the rate constant of the pseudo-first-order adsorption process (min^{-1}).

By plotting a graph of log (q_e - q_t) versus time (t), we can calculate k_1 and q_e by using slope and intercept values respectively. Fig.4 represents the pseudo first order kinetic plot for S-Alizarin red dye removal from aqueous solution.

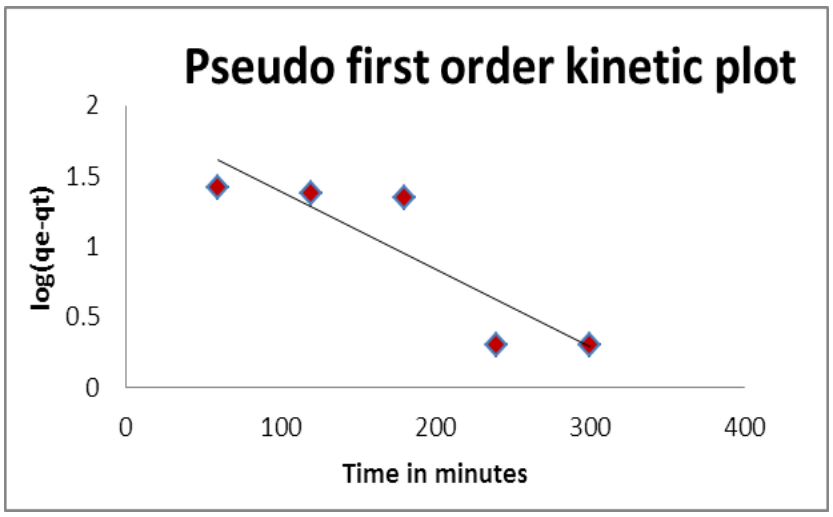

Fig. 4: Pseudo-first-order sorption kinetic plot for adsorption of S- Alizarin red dye removal from aqueous solution using nanochitosan/iron oxide nanoparticles/tamarind shell blend.

Pseudo second order equation

Due to charge transfer process between the adsorbent and adsorbate, the adsorption process takes place through the chemical interaction/ bonding. In other words we can say that this

pseudo second order kinetic model assumes that the rate limiting step is chemisorption in nature. The mechanism behind this pseudo second order kinetic plot is that it might involve valence forces by sharing or through the exchange of electrons between adsorbent and adsorbate.[29] Pseudo-second order rate equation is given as follows:

$$\frac{t}{q_t} = \frac{1}{h} + \frac{t}{q_e} \quad \text{----(2)}$$

Where $h = k_2 q_e^2$ (mg $g^{-1}min^{-1}$) can be regarded as the initial adsorption rate as *t* tends to 0 and k_2 is the rate constant of second order rate constant of adsorption process (g $mg^{-1}min^{-1}$). If pseudo-second-order kinetics is applicable, it should give a straight line and the values of second order rate constant (k_2), the equilibrium adsorption capacity (q_e) were determined from the slope and intercept of plot t /q_t versus time (t) respectively. The pseudo second order kinetic plot obtained for the removal of S- Alizarin red dye from aqueous solution was represented in Fig.5.

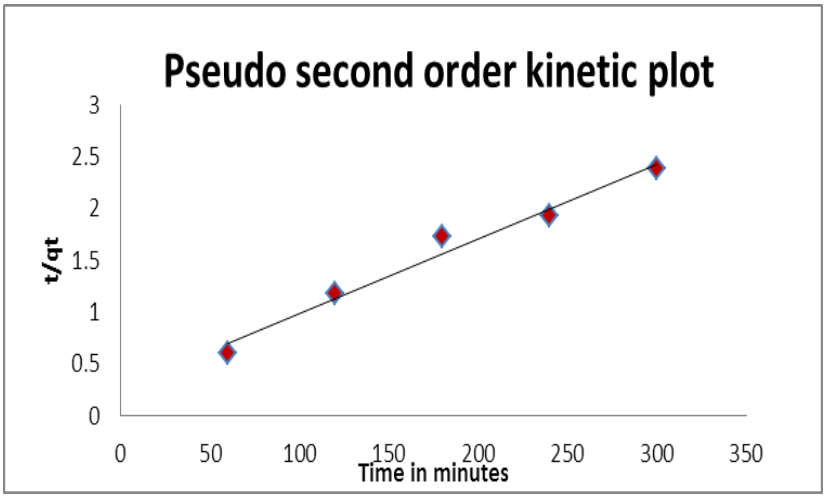

Fig.5: Pseudo-second-order sorption kinetic plot for adsorption of S- Alizarin red dye removal from aqueous solution using nanochitosan/iron oxide nanoparticles/tamarind shell blend.

The calculated values of the pseudo-first-order rate constant, pseudo-second-order rate constant and the equilibrium adsorption capacity along with the corresponding correlation coefficients determined from plots represented in Fig.4 and Fig.5 was presented in Table-1.

Table-1: Comparison between Lagergren pseudo-first-order and pseudo-second-order kinetic models for S-Alizarin Red dye sorption by nanochitosan/iron oxide nanoparticles/tamarind shell blend.

Sample	Pseudo-first-order kinetic model			Pseudo-second-order kinetic model		
	qe (mg/g)	k_1(min^{-1})	R^2	qe (mg/g)	k_2 (g mg^{-1} min^{-1})	R^2
NCS/Fe nanoparticles/ tamarind shell blend	87.116	0.01267	0.7825	138.89	0.00019	0.9761

The observed results showed that the corresponding correlation coefficients (R^2) for the pseudo second order model (correlation coefficient, R^2 = 0.9761) was found to be greater than that of the pseudo first-order model (correlation coefficient, R^2 = 0.7825) and in addition it was also identified that the pseudo second order kinetic model yield a very good straight line when compared to the pseudo first order kinetic model. Results suggested the better applicability of the pseudo-second-order model to describe the adsorption process[30], indicating that the process is controlled by chemisorptions.[31] Thus from the above obtained results it was concluded that the adsorption of S-Alizarin red dye onto nanochitosan/iron oxide nanoparticles/tamarind shell blend follows pseudo second order kinetics.

CONCLUSION

The prepared modified nanochitosan/iron oxide nanoparticles/tamarind shell blend has shown higher adsorption efficiency for the S-Alizarin dye (AY) which resulted in 75% removal. The evaluated results of effect of contact time on the adsorption efficiency indicate that the contact time of 120 minutes is enough to treat around 75% of the wastewater and kinetic studies reveals that the pseudo second order kinetic model is followed. Different interactions including the electrostatic and hydrophobic have led to the increased adsorption of the dyes onto nanochitosan/iron oxide nanoparticles/tamarind shell blend. The blend modification may also increase the capability, effectiveness and selectivity for the removal of wider range of charged pollutants including metal ions and dyes. The overall results indicate that the dye contaminated wastewater can be treated with suitably prepared modified nanochitosan/iron oxide nanoparticles/tamarind shell blend.

REFERENCES

1. Hameed BH, Ahmad AA. Batch adsorption of methylene blue from aqueous solution by garlic peel, an agricultural waste biomass. J Hazard Mater, 2009; 164: 870–875.
2. Vandana Gupta, Anupam Agarwal, Singh MK, Singh NB. Removal of Red RB Dye from Aqueous Solution by Belpatra Bark Charcoal (BBC) Adsorbent. J. Mater. Environ. Sci., 2017; 8(10): 3654-3665.
3. Gürses Ç Doğar, Yalçın M, Açıkyıldız M, Bayrak R, Karaca S. The adsorption kinetics of the cationic dye, methylene blue, onto clay. Journal of Hazard. Mater, 2006; 131: 217-228.
4. Janoš P, H. Buchtová M, Rýznarová. Sorption of dyes from aqueous solutions onto fly ash. Water Research, 2003; 37: 4938-4944.
5. Fu F, Gao Z, Gao L, Li D. Effective adsorption of anionic dye, Alizarin Red S, from aqueous solutions on activated clay modified by iron oxide. Ind Eng Chem Res., 2011; 2050: 9712–9717.
6. Bhattacharyya KG, Sharma A. Kinetics and thermodynamics of methylene blue adsorption on neem (Azadirachta indica) leaf powder. Dyes Pigment, 2005; 65: 51-59.
7. Ho YS, McKay G. Sorption of Dyes and Copper ions onto Biosorbents. Process Biochem, 2003; 38(7): 1047-1061.
8. Derbyshire F, Jagtoyen M, Andrews MR. Carbon materials in environmental applications. In: Radovic L R (eds), Chemistry and Physics of Carbon, Marcel Dekker, New York, 2001; 27.
9. Golder AK, Samanta AN, Ray S. Anionic reactive dye removal from aqueous solution using a new adsorbent- sludge generated in removal of heavy metal by electro coagulation. Chem. Eng. J., 2006; 122: 107-115.
10. Ghaedi M, Najibi A, Hossainian H, Shokrollahi A, Soylak M. Kinetic and equilibrium study of Alizarin Red S removal by activated carbon. Toxicol Environ Chem., 2012; 94(1): 40-48.
11. Oliveira LCA, Rios RVRA, Fabris JD, Garg V, Sapag K, Lago RM. Activated carbon/iron oxide magnetic composites for the adsorption of contaminants in water. Carbon, 2002; 40(12): 2177-2183.
12. Ghaedi M, Hassanzadeh A, NasiriKokhdan S. Multiwalled carbon naotubes as adsorbents for the kinetic and equilibrium study of removal of S alizarin red and morin. J Chem Eng, 2011; 56(5): 2511-2520.

13. Zhu HY, Fu YQ, Jiang R, Jiang JH, Xiao L, Zeng GM, Zhao SL, Wang Y. Adsorption removal of congo red onto magnetic cellulose/Fe_3O_4/activated carbon composite: Equilibrium, kinetic and thermodynamic studies. Chem Eng J., 2011; 173: 494.
14. Vakili MT, Rafatullah M, Salamatinia B, Zuhairi Abdullah A, Hakimi Ibrahim M, Tan KB,Gholami Z, Amouzgar P. 2014. Application of chitosan and its derivatives as adsorbents for dye removal from water and wastewater: A review. Journal of Carbohydrate Polymer, 2014; 113: 115-130.
15. Razavi, Rezaei H, Shahbazi A. Removal of Congo red from aqueous solutions using nano-chitosan. Env. Resour. Res., 2017; 5(1): 26-34.
16. Cheung WH, Szeto YS, McKay G. Enhancing the adsorption capacities of acid dyes by chitosan nano particles. Bioresour. Technol, 2009; 100: 1143–1148.
17. Ahalya N, Chandraprabha MN, Kanamadi RD, Ramachandra TV. Adsorption of methylene blue and amaranth onto tamarind pod shells. J. Biochem. Tech, 2012; 3(5): S189-S192.
18. Li-Ming Zhao, Lu-E Shi, Zhi-Liang Zhang, Jian-Min Chen, Dong-Dong Shi, Jie Yang, Zhen-Xing Tang. Preparation and application of chitosan nanoparticles and nanofibers. Brazilian Journal of Chemical Engineering, 2011; 28(03): 353–362.
19. Priscilla Prabhavathi S, Punitha J, Shameela Rajam P, Ranjith R, Suresh G, Mala N, Maruthamuthu D. Simple methods of synthesis of copper oxide, zinc oxide, lead oxide and barium oxide nanoparticles. J. Chem.Pharm. Res., 2014; 6(3): 1472-1478
20. Yu JH, Du YM, Zheng H. Blend films of chitosan gelation. Wuhan Univ J Nat Sci., 1999; 45: 440-4
21. Govindarajan C, Ramasubramaniam S, Gomathi T, Narmadha Devi A and Sudha PN. Sorption studies of Cr (VI) from aqueous solution using nanochitosan-carboxymethyl cellulose blend. Arch. Appl. Sci. Res., 2011; 3: 127-138.
22. Jahit IS, Nazmi NNM, Isa MIN and Sarbon NM. Preparation and physical properties of gelatin/CMC/chitosan composite films as affected by drying temperature. Int. Food. Res. J, 2016; 23: 1068-1074.
23. Mohammadpour Dounighi N, Eskandari R, Avadi MR, Zolfagharian H, Mir Mohammad Sadeghi A, Rezayat M. Preparation and in vitro characterization of chitosan nanoparticles containing Mesobuthus eupeus scorpion venom as an antigen delivery system. The Journal of Venomous Animals and Toxins including Tropical Diseases, 2012; 18(1): 44-52.

24. Ahalya N, Kanamadi R D, Ramachandra T V. Biosorption of Chromium (VI) by Tamarindus indica pod shells. J.Env. Sci. Res. Int, 2008; 1(2): 77-81.
25. Sedigheh Kamran, Neda Amiri Shiri. A Comparative Study for Adsorption of Alizarin Red S from Aqueous Samples by Magnetic Nanoparticles of Fe_3O_4, $CoFe_2O_4$ and Ionic Liquid-Modified Fe_3O_4. Chemical technologies, 2018; Article in Press.
26. Ashtoukhy ESZE. Loofa egyptiaca as a novel adsorbent for removal of direct blue dye from aqueous solution. J. Environ. Manage, 2009; 90(8): 2755–2761.
27. Sulaymon AH, Abood WM, Al- Musawi TJ, Ali DF. Single and Binary Adsorption of Reactive Blue and Red Dyes Onto Activated Carbon. Inter. J. Eng. Innov. Res, 2014; 3(5): 642-649.
28. Thimmasandra Narayan Ramesh, Ashwathaiah Ashwini, Devarahosahally Veeranna Kirana. Removal of Alizarin Red Dye Using Calcium Hydroxide as a Low-cost Adsorbent. J. Appl. Chem. Res., 2016; 10(1): 35-47.
29. Lagergren S. Zur theorie der sogenannten adsorption gelöster stoffe. Kungliga Svenska Vetenskapsakademiens. Handlingar, 1898; 24(4): 1-39.
30. Wasan T Al-Rubayee, Omar F Abdul-Rasheed and Noor Mustafa Ali. Preparation of a Modified Nanoalumina Sorbent for the Removal of Alizarin Yellow R and Methylene Blue Dyes from Aqueous Solutions. Hindawi Publishing Corporation, J. Chem., 2016. Article ID 4683859, 12 pages.
31. Santhi T, Manonmani S, Smitha T. Removal of malachite green from aqueous solution by activated carbon prepared from the epicarp of Ricinus communis by adsorption. J. Hazard. Mater, 2010; 179(1–3): 178–186.